9-2021

Comparison of Whole-Head Functional Near-Infrared Spectroscopy With Functional Magnetic Resonance Imaging and Potential Application in Pediatric Neurology

Julie C. Wagner
Marquette University

Anthony Zinos
Marquette University

Wei-Liang Chen
University of Washington Medical Center

Lisa Conant
Medical College of Wisconsin

Marsha Malloy
Medical College of Wisconsin

See next page for additional authors

Pediatric Neurology, Vol. 122, (September 2021): 68-75. DOI.

Comparison of Whole-Head Functional Near-Infrared Spectroscopy with Functional Magnetic Resonance Imaging and Potential Application in Pediatric Neurology

Julie C. Wagner
Department of Biomedical Engineering, Marquette University and Medical College of Wisconsin, Milwaukee, Wisconsin
Anthony Zinos
Department of Biomedical Engineering, Marquette University and Medical College of Wisconsin, Milwaukee, Wisconsin
Department of Neurology, Medical College of Wisconsin, Milwaukee, Wisconsin
Wei-Liang Chen
School of Medicine, University of Washington Medical Center and Seattle Children's Hospital, Seattle, Washington
Lisa Conant

Department of Neurology, Medical College of Wisconsin, Milwaukee, Wisconsin
Marsha Malloy
Department of Neurology, Medical College of Wisconsin, Milwaukee, Wisconsin
Department of Neurology, Children's Hospital of Wisconsin, Milwaukee, Wisconsin
Joseph Heffernan
Department of Neurology, Medical College of Wisconsin, Milwaukee, Wisconsin
Brendan Quirk
Department of Neurology, Medical College of Wisconsin, Milwaukee, Wisconsin
Jeffrey Sugar
Department of Neurology, Medical College of Wisconsin, Milwaukee, Wisconsin
Robert Prost
Department of Neurology, Medical College of Wisconsin, Milwaukee, Wisconsin
Julian B. Whelan
Department of Neurology, Medical College of Wisconsin, Milwaukee, Wisconsin
Department of Neurology, Children's Hospital of Wisconsin, Milwaukee, Wisconsin
Scott A. Beardsley
Department of Biomedical Engineering, Marquette University and Medical College of Wisconsin, Milwaukee, Wisconsin
Harry T. Whelan
Department of Neurology, Medical College of Wisconsin, Milwaukee, Wisconsin
Department of Neurology, Children's Hospital of Wisconsin, Milwaukee, Wisconsin

Abstract

Background

Changes in cerebral blood flow in response to neuronal activation can be measured by time-dependent fluctuations in hemoglobin species within the brain; this is the basis of functional magnetic resonance imaging (fMRI) and functional near-infrared spectroscopy (fNIRS). There is a clinical need for portable neural imaging systems, such as fNIRS, to accommodate patients who are unable to tolerate an MR environment.

Objective

Our objective was to compare task-related full-head fNIRS and fMRI signals across cortical regions.

Methods

Eighteen healthy adults completed a same-day fNIRS-fMRI study, in which they performed right- and left-hand finger tapping tasks and a semantic-decision tones-decision task. First- and second-level general linear models were applied to both datasets.

Results

The finger tapping task showed that significant fNIRS channel activity over the contralateral primary motor cortex corresponded to surface fMRI activity. Similarly, significant fNIRS channel activity over the bilateral temporal lobe corresponded to the same primary auditory regions as surface fMRI during

the semantic-decision tones-decision task. Additional channels were significant for this task that did not correspond to surface fMRI activity.

Conclusion

Although both imaging modalities showed left-lateralized activation for language processing, the current fNIRS analysis did not show concordant or expected localization at the level necessary for clinical use in individual pediatric epileptic patients. Future work is needed to show whether fNIRS and fMRI are comparable at the source level so that fNIRS can be used in a clinical setting on individual patients. If comparable, such an imaging approach could be applied to children with neurological disorders.

Keywords

fNIRS, fMRI, Motor cortex, Auditory cortex, Functional cortical activity

Introduction

Neuronal activation in the brain correlates with increased cerebral blood flow and volume to meet metabolic demand.[1] Changes in cerebral blood flow in response to neuronal activation, referred to as the hemodynamic response, can be measured by time-dependent fluctuations in oxygenation of hemoglobin species within the brain. This neurovascular coupling is the basis of many functional neuroimaging techniques, including functional magnetic resonance imaging (fMRI), positron emission tomography (PET), single-photon emission computerized tomography (SPECT), and functional near-infrared spectroscopy (fNIRS).

fNIRS is a noninvasive imaging tool that uses changes in near-infrared light absorbance to measure changes in oxygenated and deoxygenated hemoglobin concentrations and assess regional tissue oxygenation.[2] First described by Jöbsis 40 years ago,[3] fNIRS has been used clinically for monitoring regional oxygenation, for example, in pediatric intensive care units,[4,5] but it has not been widely utilized in clinical neurology and the neurosciences.[6,7] The portability and cost-effectiveness of fNIRS relative to other functional neuroimaging modalities, such as fMRI, has attracted clinicians and neuroscientists to explore the feasibility of using fNIRS as an alternative approach to assess neurovascular integrity and brain function. fNIRS can be easily set up at bedside without the need to transport patients, which is particularly crucial for critically ill children whose care requires immobilization. Importantly, fNIRS has the unique ability to monitor brain activity continuously in real time, which can be especially relevant in pediatric populations. Continuous assessment of brain activity can not only help researchers to establish a deeper physiologic understanding of the developing brain but also can help clinicians derive important diagnostic and prognostic biomarkers for different common pediatric pathologies, such as epilepsy,[8] hypoxic-ischemic encephalopathy,[9] and traumatic brain injury.[10,11]

To show how clinically useful fNIRS can be, recent studies have focused on using group analysis to validate fNIRS with fMRI at the channel[12,13] and source levels.14, 15, 16 Source-level comparisons during median nerve stimulation have shown spatial and amplitude correlations between fNIRS and fMRI with $|R| > 0.48$ and > 0.5, respectively.[14] Similarly, for more complicated tasks, Hernández-Martin and colleagues[15] reported up to 60% overlap between fNIRS and fMRI within frontal regions of interest

when subjects did mathematical calculations. Wijeakumar and colleagues[16] also found correlations ($R > 0.6$) between fNIRS and fMRI during a working memory task. In these validation studies, fNIRS optodes were concentrated on a specific region of interest, limiting spatial comparisons of functional activity only to regions where activity was expected. To be clinically useful, fNIRS needs to show comparable detection of functional activity across the whole cortical surface.

We compared fNIRS detection of task-related activity across cortical areas to fMRI. As fNIRS measures the same physiological response as fMRI,[17] activation patterns should be similar at the group level across the two modalities. Performing this first full-head assessment is an important step toward demonstrating the clinical utility of fNIRS.

Materials and Methods

Participants

After a screening process wherein subjects performed structured tasks to determine if a strong task-related hemodynamic response was detectable with fNIRS, 20 healthy adults participated in a same-day fNIRS-fMRI study; however, one participant terminated the fMRI session early and another terminated the fNIRS session early. Data for the remaining 18 participants (38.9 ± 15.1 years, 6 male) were analyzed. All participants were right-handed based on the Edinburgh Handedness Survey,[18] had normal or corrected to normal vision, and utilized English as their native language. The study was approved by the Medical College of Wisconsin Institutional Review Board, and informed consent was obtained for all subjects prior to participation.

Experimental equipment

fNIRS data were collected using a continuous wave optical system at 760 and 850 nm with a sampling frequency of 3.125 Hz. All fNIRS data were collected using the NIRScoutX (NIRx Medical Technologies, Glen Head, NY, USA) with NIRStar (ver 15-2). To capture full-head imaging, 32 emitters and 32 detectors were placed about the scalp with an interoptode distance of approximately 3 cm for a total of 102 channels. Subject-specific channel locations and anatomical landmarks were digitized using a Polhemus FastTrack system (Polhemus, Colchester, VT, USA). Figure 1 depicts how the average montage and resulting channels are placed over various anatomical regions. During fNIRS testing, participants sat upright in a darkened room while viewing a 44-cm computer display placed at eye level approximately 60 cm away.

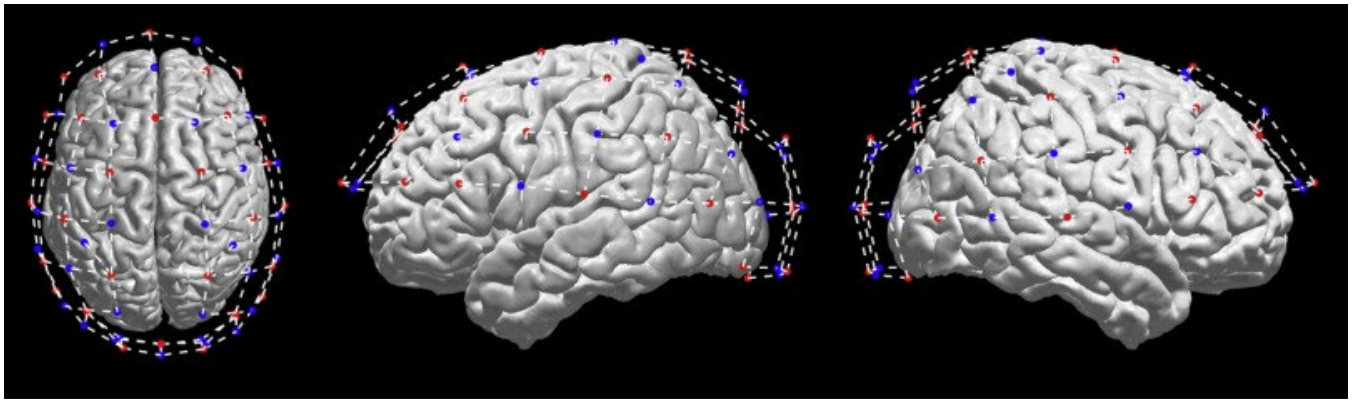

FIGURE 1. Functional near-infrared spectroscopy probe montage. Emitters (32) are shown as red circles, and detectors (32) are shown as blue circles. The resulting channels are shown as dashed white lines. The probe montage is placed over the Colin27 brain to show which anatomical features are beneath various channels.

Functional and structural MR images were obtained using a GE Healthcare 3T Signa Premier scanner. High-resolution whole-brain anatomical images were obtained at the beginning of the imaging session using T1-weighted gradient recall images (176 slices, repetition time = 8 ms, echo time = 3.1 ms, flip angle = 12°, 1 × 1 × 1 mm voxels). Functional MR images consisted of axially oriented T2∗-weighted echo planar images covering the whole brain (41 slices, repetition time = 2.0 seconds, echo time = 23 ms, flip angle = 77°, 3.5 × 3.5 × 3.5 mm voxels). The number of functional volumes varied for each task: 205 for the motor task and 274 for the language task. During the fMRI session, participants wore the cap used during fNIRS data acquisition with vitamin E capsules placed in the channel locations to verify channel registration on the participant's head.

Experimental tasks

Participants took part in same-day fNIRS and fMRI experimental sessions in which they completed separate tasks assessing motor and language function. Each task was presented in a block paradigm consisting of task periods interleaved with rest periods. Motor cortices were functionally localized using a sequential finger tapping task (i.e., Motor task) in which participants tapped their thumb to each finger starting with their index finger going toward their little finger and then reversed the sequence as fast as possible while still hitting each individual digit. While the word RIGHT or LEFT was displayed on the screen (20 seconds), participants sequentially tapped the fingers on their corresponding hand. Following each tapping sequence participants were presented with a 20-second rest period and asked to fixate on a crosshair placed at the center of the screen while performing no movement. Participants completed 10 cycles of the motor task for each hand.

To identify language-related functional regions, the Semantic-Decision Tone-Decision (SDTD) paradigm developed by Binder and colleagues was implemented.19, 20, 21 Briefly, the paradigm consisted of two conditions. During the tone decision control condition (Tone task), participants heard a series of high- and low-pitch tone sequences. Each sequence varied in length between three and seven consecutive tone presentations and consisted of at most two high-pitch (750 Hz) target tones presented within a sequence of low-pitch (500 Hz) tones. Participants were asked to press a button if two high-pitch tones were presented in the sequence of tones. For the semantic decision condition (Semantic task), participants heard the names of animals and were asked to press a button if the animal was both “found in the United States,” not including zoos, and “used by humans.” Sequences of eight stimuli (consisting of either tones or animal names) were presented in separate 28 second blocks followed by 17.5 seconds of rest for a total of 12 cycles per task condition.

Experimental presentations of the task sequences and stimuli were carried out using PsychoPy3.[22] The order of experiments and the tone and animal name sequence order were randomly chosen for each experimental session. In addition, before starting the functional tasks in the fNIRS session, baseline brain activity was measured during a five-minute period while participants looked at a black screen in a restful wakeful state.

For both fMRI and fNIRS, the individual tasks (i.e., Right, Left, Semantic, and Tone) were analyzed as were the contrasts between conditions within a functional task. For the Motor task, the Right-hand condition was contrast with Left-hand condition (Right-Left) to highlight motor regions specific to each hand. For the SDTD task, the Semantic decision condition was contrast with the Tone decision condition (Semantic-Tone) to identify language processing regions. The Semantic-Tone contrast produces highly reliable, left-lateralized activation in frontal, temporal, and parietal regions previously implicated in language processing.

Data analysis

fNIRS

All fNIRS data analysis was completed using MATLAB R2018b (Mathworks, Natick, MA, USA), using the NIRS Brain Analyzer Toolbox.[23] Before analysis, the raw light absorbance data were converted into optical densities. Artifacts related to head movements during experiments were removed using temporal derivative distribution repair motion correction.[24] Signals were iteratively weighted based on how much a sampled time point varied from the standard deviation of the entire signal. Weighting continued until the channel average converged.

Following motion correction, the optical density of each channel was converted into separate oxyhemoglobin (HBO) and deoxyhemoglobin (HBR) states using the Beer-Lambert law.[25] Scalp blood flow was removed using principal component analysis applied over the entire time series for each channel. Based on results from Zhang and colleagues,[26] the first principal component analysis component reliably captures scalp blood flow and was thus subtracted from the channel time series data.

fMRI

All fMRI processing was performed using fMRIPrep 1.4.1,[27] which is based on Nipype 1.2.0.[28] Briefly, all anatomical scans were corrected for intensity nonuniformity, skull stripped, segmented, and normalized to standard space (MNI152NLin2009cAsym). Brain surfaces were reconstructed using recon-all (FreeSurfer 6.0.1).[29] All functional scans were corrected for susceptibility distortions using two echo planar imaging references with opposing phase-encoding directions, coregistered to the T1-weighted image, motion corrected, normalized to standard space, and smoothed with a 4-mm full width at half maximum Gaussian kernel.

Comparison between fNIRS and fMRI

Group volumetric results were projected to the cortical surface using the ribbon constraint surface mapping method in Connectome Workbench[30] as described by Glasser and colleagues.[31] Briefly, a gray matter ribbon was created from the white matter and pial segmented surfaces of the Colin27 brain. Sampled volumetric data from voxels nearby the gray matter ribbon were weighted based on how well they fell within the ribbon and used to estimate the cortical surface activity. The projection of fMRI activity onto the cortical surface was used to visualize the regions of significant activity that can be detected with fNIRS when overlaying the coregistered channel results.

The group-average fNIRS probe montage from all subjects was coregistered to the Colin27 brain and used to display channel results. The average probe montage was created by first aligning the measured probe locations for each participant to their corresponding anatomy. Next, a single-probe montage

was chosen as a reference and the montages for the remaining participants were aligned using an affine transformation estimated via least squares to map a set of 13 fiducial points. Following alignment to the reference, the average location of each sensor was computed. The Colin27 cortical mesh was then aligned to the average probe location in NIRS Brain Analyzer Toolbox using the fiducial points. A custom database written in Python was used to store the primary datasets in a fully deidentified format.

Statistics

fNIRS

A general linear model (GLM) was used to determine whether the neurological response of a given channel was associated with a task. An autoregressive (AR) prewhitening filter and iteratively reweighted least squares were used during the GLM analysis,[32] to remove serially correlated physiological noise and any motion artifacts not accounted for by the temporal derivative distribution repair analysis. Specifically, the GLM model was given by:

(1)

$$y = X\beta + \varepsilon$$

where *y* is the measured hemodynamic data, *X* is the design matrix defined by the convolution between the stimulus block and the canonical hemodynamic response function, and ε is assumed to be normally distributed ($\sim N(0,\sigma^2)$) noise. Model coefficients, β, were initialized by inverting *X* via ordinary least squares method. The model was then iteratively solved to remove serially correlated noise by fitting the model residual $y - X\beta$ to an AR model. The resulting AR coefficients were used to generate a prewhitening filter, which was then applied to the hemodynamic data and design matrices. The GLM was then refit and the process repeated until changes in β were less than 1%. For details on AR prewhitening and the iteratively reweighted least squares process see Refs. 32,33.

A second-level analysis was applied at the group level using a mixed effects model to determine whether functional activity was present across participants:

(2)

$$\beta = A \cdot \Gamma$$

were β is the beta weights from the first-level GLM analysis of each participant, *A* is the mixed effects model, and Γ are the task conditions. Additional regressors such as age and gender were not included in the model. A *t* test was computed using the beta weights and corrected for multiple comparisons across fNIRS channels using the Benjamini-Hochberg method.[34]

fMRI

First-level BOLD signal changes for each task were analyzed in the Analysis of Functional NeuroImaging program AFNI 20.2.19[35] using a GLM with restricted maximum likelihood estimate model (*3dREMLfit*) to estimate temporal autocorrelations. Stimulus regressors were created for each task condition by convolving the stimulus onset with a duration modulated block. Six motion parameters were included as covariates of no interest. Second-level group analysis was performed with *3dttest++* using the contrasts of interest between regressors' parameter maps for each participant

as input. Regions of significant functional activity were defined using a voxelwise $P < 0.001$ threshold and provided as input to *3dClustSim* to determine the minimum cluster size (0.94 mL) to achieve a corrected significance of $P < 0.05$. Group-level results were mapped to the Colin27 brain[36] for visualization.

Results

fNIRS

Contralateral somatosensory and motor cortex activation was significant for Right ($t(18) = 2.62$; $P < 0.05$) and Left ($t(18) = 2.68$; $P < 0.05$) finger tapping conditions for both hemoglobin states (Fig 2A and B). Specifically, there was an increase in HBO and decrease in HBR for these regions. Furthermore, for the Left condition, ipsilateral motor channels were also significant ($t(18) = 2.96$, $P < 0.05$). When the contrast was applied (Fig 2C), there was a significant ($t(18) = 3.74$; $P < 0.05$) increase in HBO in the left somatosensory/motor cortex for the Right relative to Left condition. Similarly, right somatosensory/motor cortex showed greater activation (represented by the blue cluster, Fig 2C) for the Left relative to Right condition. Adjacent channels within these regions were just under the significance threshold. Because there was bilateral activity present in the Left HBR condition whose magnitude was similar to the Right HBR condition, the contrast resulted in no significant channels. Similar to the HBO result, somatosensory and motor region channels for both hemispheres in the contrast were just below the corrected significance threshold ($t(18) = [2.16\ 3.09]$).

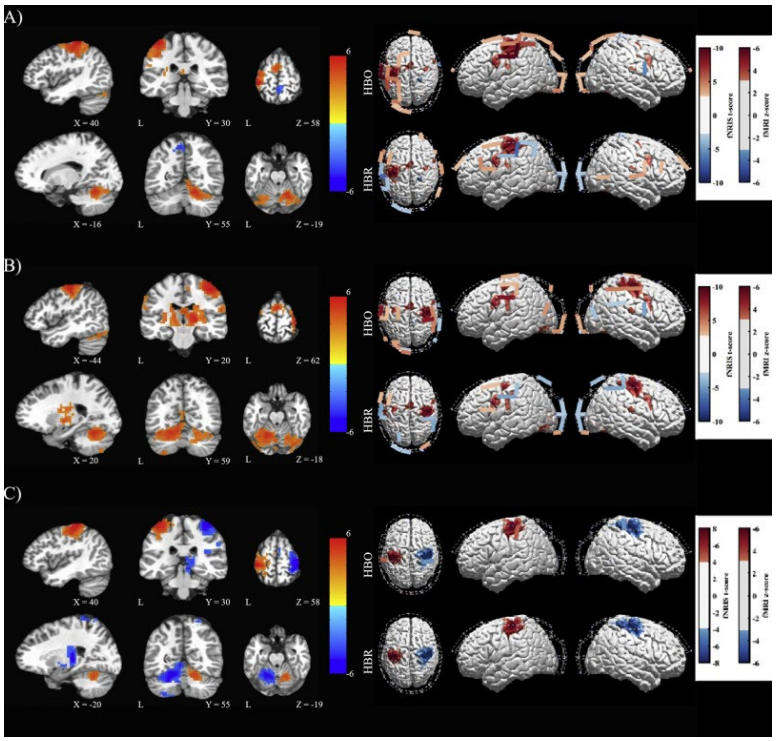

FIGURE 2. Motor Task. Group-level (N = 18) Motor task results for functional near-infrared spectroscopy (fNIRS) (right) and functional magnetic resonance imaging (fMRI) (radial coordinates) separated into Right (A), Left (B), and the contrast Right-Left (C) hand finger tapping. Volumetric fMRI results (left) highlight the most significant voxels for primary motor clusters (top) and cerebellar clusters (bottom) for each condition (voxelwise threshold $P < 0.001$ cluster corrected at $P < 0.05$). Channel fNIRS (group average probe montage shown) show oxyhemoglobin (top) and deoxyhemoglobin (bottom) results displayed as *t* scores with a corrected

threshold ($P < 0.05$) overlayed on top of the surface fMRI *z* score results thresholded at $P < 0.001$. All fMRI results are displayed on the Colin27 brain.

Channels over the bilateral temporal regions showed an increase in HBO and decrease in HBR for both Semantic ($t(18) = 2.40$; $P < 0.05$) and Tone ($t(18) = 2.39$; $P < 0.05$) conditions (Fig 3A and B). When the contrast was applied (Fig 3C), a significant increase in HBO ($t(18) = 2.81$; $P < 0.05$) was seen in channels over the frontal and parietal lobes of left hemisphere for the Semantic relative to Tone condition. Increased channel activity over the primary auditory cortex in the right hemisphere was seen with respect to the Tone relative to Semantic condition.

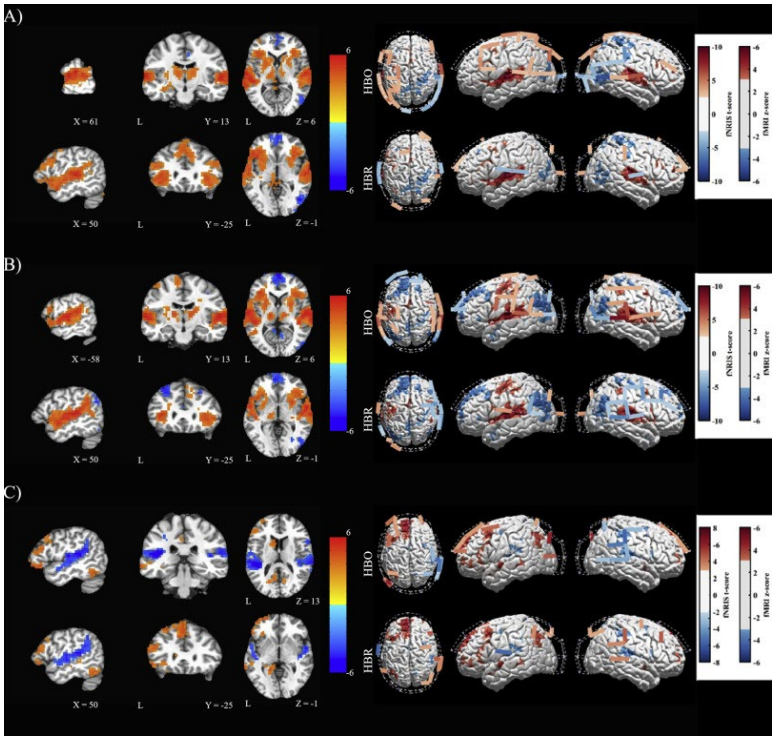

FIGURE 3. Language Task. Group-level (N = 18) Semantic-Decision Tone-Decision task results for functional near-infrared spectroscopy (fNIRS) (right) and functional magnetic resonance imaging (fMRI) (radial coordinates) separated into Semantic (A), Tone (B), and the contrast Semantic-Tone (C) auditory presentations. Volumetric fMRI results (left) highlight the most significant voxels for primary auditory clusters (top) and over the inferior frontal gyrus (bottom) for each condition (voxelwise threshold $P < 0.001$ cluster corrected at $P < 0.05$). Channel fNIRS (group average probe montage shown) show oxyhemoglobin (top) and deoxyhemoglobin (bottom) results displayed as *t* scores threshold with a corrected threshold ($P < 0.05$) overlayed on top of the surface fMRI *z* score results thresholded at $P < 0.001$. All fMRI results are displayed on the Colin27 brain.

fMRI

Similar to fNIRS, fMRI results showed significant contralateral somatosensory and motor activity during Right and Left finger tapping conditions as well as cerebellar activity (Fig 2A and B). For the Right condition, peak cluster activity occurred over the left postcentral gyrus ($z = 6.51$; $P < 0.001$) and right cerebellum lobes VI ($z = 5.62$; $P < 0.001$) whereas for the Left condition, peak cluster activity occurred over the right precentral gyrus ($z = 6.37$; $P < 0.001$) and left cerebellum lobe VI ($z = 5.51$; $P < 0.001$). During the Left condition, significant ipsilateral motor activation was also

observed over the precentral gyrus (z = 4.53.29; P < 0.001). For the Right-Left contrast (Fig 2C), there was significantly greater activation in the left motor cortex (z = 6.65; P < 0.001) and right cerebellum (z = 4.96; P < 0.001) in the Right condition relative to the Left, whereas greater activation was seen in the right motor cortex (z = 6.68; P < 0.001) and left cerebellum (z = 5.66; P < 0.001) for the Left relative to the Right.

Peak significant fMRI cluster activity for the SDTD task occurred in the superior temporal gyri for Semantic (left: z = 6.38; right: z = 5.96; P < 0.001) and Tones (left: z = 6.68; right: z = 6.34; P < 0.001) conditions (Fig 3A-B). For the Semantic-Tone contrast (Fig 3C), greater activation was present in the left superior, middle, and inferior frontal gyri (z = 4.05; P < 0.001) as well as the left superior temporal sulcus and inferior temporal gyrus for the Semantic relative to Tone condition, whereas increased activation was present in bilateral superior temporal gyri (left: z = 6.05; right: z = 5.36; P < 0.001) for the Tone relative to Semantic condition.

fNIRS versus fMRI

fNIRS HBO and HBR channels over somatosensory/motor cortex measured significant task-related activity over the same clusters as the fMRI surface projection (Fig 2A and B) for both Right and Left conditions. The strongest detection occurred for the HBO Right condition, with five channels overlapping the cluster, whereas two channels each for HBR Right and HBO Left conditions overlapped with the fMRI cluster. Ipsilateral motor cortex was also detected in two channels for the Left HBO and HBR conditions, which corresponded spatially with the three smaller fMRI clusters within that region. Due to similarities between individual Right and Left conditions, the somatosensory and motor fMRI clusters were detected by a single HBO channel in each hemisphere for the Right-Left contrast (Fig 2C).

For the SDTD task, bilateral temporal activity was detected in both Semantic and Tones HBO and HBR conditions that overlapped with the corresponding fMRI clusters (Fig 3A and B). Additional fNIRS channels with significant activity were not associated with the surface fMRI activity, such as the left motor cortex in the HBO Semantic condition. Furthermore, when the contrast was applied, greater activation for the Semantic relative to Tone HBO channels could detect the left superior frontal gyrus fMRI clusters, whereas greater activation for Tone relative to Semantic HBO detected the fMRI cluster in the right temporal gyrus (Fig 3C). fMRI activity in the left inferior frontal gyrus was not detected with the contrast.

Discussion

In this study, full-head fNIRS was compared with same-day fMRI in 18 subjects while performing Motor and Language tasks. We found overlap between channel HBO and HBR fNIRS results and surface-projected fMRI results for all tasks, especially the Motor task, at the group level. These results suggest that whole-head fNIRS is comparable to fMRI in detecting task-related cortical hemodynamic changes across lateral cortex.

It has been well demonstrated by other groups that regional hemodynamic changes can be detected by fNIRS.12, 13, 14, 15, 16,[37] For example, Huppert and colleagues[37] reported a Pearson's correlation of 0.7 and 0.98 between changes in the fMRI BOLD response and fNIRS HBO and HBR changes respectfully during a right-hand finger tapping task when fNIRS optodes were placed only over the contralateral hemisphere. Other more recent studies have shown a similar correlation (r > 0.5) with

fMRI during simple visual or motor tasks.[12,16,]37, 38, 39 Because these tasks produce a large physiological response, corresponding regional fNIRS findings are expected. What is unique in our current study is the use of whole-head fNIRS to detect task activity across lateral cortex in both hemispheres. Even though Huppert and colleagues reported similar contralateral results to ours, their regional approach could not detect the task-related activity reported here in the ipsilateral hemisphere; this becomes even more relevant in clinical settings where neural network dynamics may be more variable.

Although most validation studies have been performed using visual or motor tasks, optical imaging can also be used to measure cortical activity for auditory and language processing. Eggebrecht and colleagues[40] used diffuse optical tomography (DOT) with language-related tasks and compared their source-level spatial results with fMRI using spatial correlations. For the hearing words portion of their language task, they reported significant HBO and HBR sources over bilateral superior temporal regions similar to our fNIRS channel and fMRI results for both Semantic and Tone tasks. The investigators also found that when the fMRI data were smoothed to the same resolution as DOT, HBO and HBR were strongly spatially correlated with fMRI in bilateral visual and auditory regions associated with reading (0.86 and 0.83 for HBO and HBR, respectively) and hearing (0.63 and 0.68 for HBO and HBR, respectively) words but correspondence was more limited on their convert verb generation task (0.32 and 0.22 for HBO and HBR, respectively).[40] Combined with our results, this indicates how optical imaging can be useful in detecting regions of general auditory processing, but analytical advancement is still necessary to identify language processing regions at the same level as fMRI. The potential to detect and spatially localize motor, auditory, and language processing is clinically significant. Language mapping has been difficult when it comes to pediatric patients. Invasive procedures, such as the Wada test, subject the patient to substantial risk. With the continued advancement of fNIRS systems and analysis techniques, optical imaging could be used as an alternative tool for language mapping.

At present, fNIRS systems have limited spatial resolution, especially with respect to fMRI or DOT.[40,41] Despite this, the channel-wise comparison, shown here across tasks, suggests that fNIRS can detect functional activity across the lateral cortices. Detailed validation of the spatial sensitivity across brain networks will require source analysis at the single subject level. Another inherent limitation of fNIRS to fMRI is the lower signal-to-noise ratio.[38] The lower signal-to-noise ratio inherent to fNIRS could partially explain why the Right-Left HBR contrast did not reveal significant activity as somatosensory and motor cortex channels were just under threshold. Furthermore, some fNIRS channels did not align fully with the central point of the fMRI clusters; this is due in part to the estimation of source and detector locations required for the group analysis. Because the current analysis was performed at the group level, there was no single set of measured locations for the group. Therefore, the group average of coregistered sensor locations was used to display the results. This group montage generates location uncertainties of up to 4 mm S.D. in all directions. For analyses performed at the individual subject level, these inaccuracies would be removed and make it possible to coregister the channel montage and fMRI activity to the individual anatomy.

Conclusion

We were able to detect significant task-related group-level activity in fNIRS channels located over fMRI clusters for a simple motor task as well as primary auditory cortices during a more complicated

semantic processing task in healthy adults. These results are an important first step toward individual subject analysis that can be applied at the clinical level, such as with pediatric patients with epilepsy.

Acknowledgments

Ken Swaiman was truly one of the founders of child neurology. We all stand upon his shoulders, as we reach to advance the field we love.

References

1 P.T. Fox, M.E. Raichle. **Stimulus rate dependence of regional cerebral blood flow in human striate cortex, demonstrated by positron emission tomography.** *J Neurophysiol*, 51 (1984), pp. 1109-1120

2 M. Hiraoka, M. Firbank, M. Essenpreis, *et al.* **A Monte Carlo investigation of optical pathlength in inhomogeneous tissue and its application to near-infrared spectroscopy.** *Phys Med Biol*, 38 (1993), pp. 1859-1876

3 F.F. Jobsis. **Noninvasive, infrared monitoring of cerebal and myocardial oxygen sufficiency and circulatory parameters.** *Science*, 198 (1977), pp. 1264-1267

4 B. Balakrishnan, M. Dasgupta, K. Gajewski, *et al.* **Low near infrared spectroscopic somatic oxygen saturation at admission is associated with need for lifesaving interventions among unplanned admissions to the pediatric intensive care unit.** *J Clin Monit Comput*, 32 (2018), pp. 89-96

5 G.M. Hoffman, N.S. Ghanayem, J.P. Scott, J.S. Tweddell, M.E. Mitchell, K.A. Mussatto. **Postoperative cerebral and somatic near-infrared spectroscopy saturations and outcome in hypoplastic left heart syndrome.** *Ann Thorac Surg*, 103 (2017), pp. 1527-1535

6 H. Obrig. **NIRS in clinical neurology - a 'promising' tool?** *Neuroimage*, 85 (2014), pp. 535-546

7 K.-S. Hong, M.A. Yaqub. **Applilcation of functional near-infrared spectroscopy in the healthcare industry: a review.** *J Innov Opt Health Sci*, 12 (2019), pp. 1-91

8 P. Monrad, K. Sannagowadra, X. Bozarth, *et al.* **Haemodynamic response associated with both ictal and interictal epileptiform activity using simultaneous video electroencephalography/near infrared spectroscopy in a within-subject study.** *J Near Infrared Spectrosc*, 23 (2015), pp. 209-218

9 P. Wintermark, A. Hansen, S.K. Warfield, D. Dukhovny, J.S. Soul. **Near-infrared spectroscopy versus magnetic resonance imaging to study brain perfusion in newborns with hypoxic-ischemic encephalopathy treated with hypothermia.** *Neuroimage*, 85 (2014), pp. 287-293

10 F.A. Zeiler, J. Donnelly, L. Calviello, D.K. Menon, P. Smielewski, M. Czosnyka. **Pressure autoregulation measurement techniques in adult traumatic brain injury, part I: a scoping review of intermittent/semi-intermittent methods.** *J Neurotrauma*, 34 (2017), pp. 3207-3223

11 F.A. Zeiler, J. Donnelly, L. Calviello, P. Smielewski, D.K. Menon, M. Czosnyka. **Pressure autoregulation measurement techniques in adult traumatic brain injury, part II: a scoping review of continuous methods.** *J Neurotrauma*, 34 (2017), pp. 3224-3237

12 E. Maggioni, E. Molteni, C. Zucca, *et al.* **Investigation of negative BOLD responses in human brain through NIRS technique. A visual stimulation study.** *Neuroimage*, 108 (2015), pp. 410-422

13 D. Donizete de Faria, A.J.M. Paulo, J. Balardin, *et al.* **Task-related brain activity and functional connectivity in upper limb dystonia: a functional magnetic resonance imaging (fMRI) and functional near-infrared spectroscopy (fNIRS) study.** *Neurophotonics*, 7 (2020), pp. 1-13

14 T. Huppert, J. Baker, B. Schmidt, S. Walls, A. Ghuman. **Comparison of group-level, source localized activity for simultaneous functional near-infrared spectroscopy- magnetoencephalography**

and simultaneous fNIRS-fMRI during parametric median nerve stimulation. *Neuropathology*, 4 (2017), pp. 1-13

15 E. Hernández-Martin, F. Marcano, O. Casanova, C. Modroño, J. Plata-bello, J.L. González-mora. **Comparing diffuse optical tomography and functional magnetic resonance imaging signals during a cognitive task: pilot study.** *Neurophotonics*, 4 (2017), pp. 1-15

16 S. Wijeakumar, T.J. Huppert, V.A. Magnotta, A.T. Buss, J.P. Spencer. **Validating an image-based fNIRS approach with fMRI and a working memory task.** *Neuroimage*, 147 (2017), pp. 204-218

17 W. Chen, J. Wagner, N. Heugel, *et al.* **Functional near-infrared spectroscopy and its clinical application in the field of neuroscience: advances and future directions.** *Front Neurosci*, 14 (2020), pp. 1-15

18 R. Oldfield. **The assessment and analysis of handedness: the Edinburgh inventory.** *Neuropsychologia*, 9 (1971), pp. 97-113

19 J.R. Binder, S.M. Rao, T.A. Hammeke, *et al.* **Lateralized human brain language systems demonstrated by task subtraction funtional magnetic resonance imaging.** *Arch Neurol*, 52 (1995), pp. 593-601

20 J.K. Janecek, S.J. Swanson, D.S. Sabsevitz, *et al.* **Language lateralization by fMRI and Wada testing in 229 patients with epilepsy: rates and predictors of discordance.** *Epilepsia*, 54 (2013), pp. 314-322

21 J.R. Binder, S.J. Swanson, T.A. Hammeke, D.S. Sabsevitz. **A comparison of five fMRI protocols for mapping speech comprehension systems.** *Epilepsia*, 49 (2008), pp. 1980-1997

22 J. Peirce, J.R. Gray, S. Simpson, *et al.* **PsychoPy2: experiments in behavior made easy.** *Behav Res Methods*, 51 (2019), pp. 195-203

23 H. Santosa, X. Zhai, F. Fishburn, T. Huppert. **The NIRS brain AnalyzIR toolbox.** *Algorithms*, 11 (2018), pp. 1-33

24 F.A. Fishburn, R.S. Ludlum, C.J. Vaidya, A.V. Medvedev. **Temporal derivative distribution repair (TDDR): a motion correction method for fNIRS.** *Neuroimage*, 184 (2019), pp. 171-179

25 S.L. Jacques. **Optical properties of biological tissues: a review.** *Phys Med Biol*, 58 (2013), pp. R37-R61

26 X. Zhang, V.Y. Toronov, A.G. Webb. **Simultaneous integrated diffuse optical tomography and functional magnetic resonance imaging of the human brain.** *Opt Express*, 13 (2005), pp. 5513-5521

27 O. Esteban, C.J. Markiewicz, R.W. Blair, *et al.* **fMRIPrep: a robust preprocessing pipeline for functional MRI.** *Nat Methods*, 16 (2019), pp. 111-116

28 K. Gorgolewski, C.D. Burns, C. Madison, *et al.* **Nipype: a flexible, lightweight and extensible neuroimaging data processing framework in Python.** *Front Neuroinform*, 5 (2011), pp. 1-15

29 A.M. Dale, B. Fischl, M.I. Sereno. **Cortical surface-based analysis I. Segmentation and surface reconstruction.** *Neuroimage*, 9 (1999), pp. 179-194

30 D.C. Van Essen, S.M. Smith, D.M. Barch, T.E.J. Behrens, E. Yacoub, K. Ugurbil
The Wu-Minn Human Connectome Project: an overview
Neuroimage, 80 (2013), pp. 62-79

31 M.F. Glasser, S.N. Sotiropoulos, J.A. Wilson, *et al.* **The minimal preprocessing pipelines for the Human Connectome Project.** *Neuroimage*, 80 (2013), pp. 105-125

32 J.W. Barker, A. Aarabi, T.J. Huppert. **Autoregressive model based algorithm for correcting motion and serially correlated errors in fNIRS.** *J Biomed Opt Express*, 4 (2013), pp. 1366-1379

33 A.E. Beaton, J.W. Tukey. **The fitting of power series, meaning polynomials, illustrated on band-spectroscopic data.** *Technometrics*, 16 (1974), p. 1747 185

34 Y. Benjamini, Y. Hochberg. **Controlling the false discovery rate: a practical and powerful approach to multiple testing.** *J R Stat Soc Ser B Methodol*, 57 (1995), pp. 289-300
35 R.W. Cox. **AFNI: software for analysis and visualization of functional magnetic resonance neuroimages.** *Comput Biomed Res*, 29 (1996), pp. 162-173
36 C.J. Holmes, R. Hoge, L. Collins, R. Woods, A. Toga, A.C. Evans. **Enhancement of MR images using registration for signal averaging.** *J Comput Assist Tomogr*, 22 (1998), pp. 324-333
37 T.J. Huppert, R.D. Hoge, S.G. Diamond, M.A. Franceschini, D.A. Boas. **A temporal comparison of BOLD, ASL, and NIRS hemodynamic responses to motor stimuli in adult humans.** *Neuroimage*, 29 (2006), pp. 368-382
38. X. Cui, S. Bray, D.M. Bryant, G.H. Glover, A.L. Reiss. **A quantitative comparison of NIRS and fMRI across multiple cognitive tasks.** *Neuroimage*, 54 (2011), pp. 2808-2821
39 T.J. Huppert. **Commentary on the statistical properties of noise and its implication on general linear models in functional near-infrared spectroscopy.** *Neurophotonics*, 3 (2016), pp. 1-10
40 A.T. Eggebrecht, S.L. Ferradal, A. Robichaux-Viehoever, *et al.* **Mapping distributed brain function and networks with diffuse optical tomography.** *Nat Photon*, 8 (2014), pp. 448-454
41 H. Obrig, A. Villringer. **Beyond the visible - imaging the human brain with light.** *J Cereb Blood Flow Metab*, 23 (2003), pp. 1-18